Available online at www.sciencedirect.com

ScienceDirect

IFAC Papers Online CONFERENCE PAPER ARCHIVE

IFAC PapersOnLine 56-2 (2023) 5615–5619

Influence of Reconstruction Algorithms on Harmonic Analysis in Electrical Impedance Tomography

Erik Stein * **Rongqing Chen** *,** **Alberto Battistel** *
András Lovas *** **Balázs Benyó** **** **Knut Möller** *

* *Institute of Technical Medicine (ITeM), Furtwangen University (HFU), Villingen-Schwenningen, Germany (e-mail: e.stein@hs-furtwangen.de).*
** *Faculty of Engineering, University of Freiburg, Freiburg, Germany*
*** *Department of Anaesthesiology and Intensive Therapy, Kiskunhalas Semmelweis Hospital, Kiskunhalas, Hungary*
**** *Budapest University of Technology and Economics, Faculty of Electrical Engineering and Informatics, Department of Control Engineering and Information Technology, Budapest, Hungary*

Abstract: Electrical Impedance Tomography (EIT) is a commonly used imaging technique for monitoring respiration on the bedside and it might have the potential for monitoring lung perfusion. Several signal processing approaches have been developed to separate respiration and perfusion. In this contribution we investigated whether different image reconstruction algorithms influence the separation results provided by the harmonic analysis approach. We compared the algorithms used by Dräger, the Gauss-Newton method with different regularizers as well as the GREIT algorithm. The comparison was carried out using a retrospective EIT dataset from a COVID-19 patient. The results gave insight that the harmonic analysis separation approach is dependent on the reconstruction algorithms. Both, the separation of the perfusion and the separation of the respiration showed differences between the reconstruction algorithms when carried out pixel-wise. On the other hand, the separations carried out on the global impedance only showed marginal differences for the separated perfusion.

Keywords: Medical imaging and processing; Developments in measurement, signal processing; Decision support and control

1. INTRODUCTION

Electrical impedance tomography is a known and might become an established imaging technique in the clinical environment. It can be used for monitoring respiration on the bedside especially of mechanically ventilated patients in intensive care units (ICU) (Frerichs et al., 2017).

Due to its measurement principle, EIT has a high temporal but low spatial resolution (Frerichs et al., 2017). Most of the time, a belt with 16 electrodes is placed around the chest of a patient (Frerichs et al., 2017; Adler and Boyle, 2017). Then, two electrodes are used for injecting an alternating current and the remaining electrode pairs are used for measuring the resulting voltages (Frerichs et al., 2017; Adler and Boyle, 2017). Subsequently, another electrode pair is used for current injection. A full measurement cycle therefore consists of 208 voltages. Because the human thorax contains tissues of different and variable conductivities, the measured voltages also differ at each electrode pair and other time (Frerichs et al., 2017; Adler and Boyle, 2017).

In EIT these voltages are used to reconstruct the tissue conductivities of the thorax. Unfortunately, EIT is an ill-posed inverse problem because the measurement space (voltage changes) is significantly smaller than the parameter space (conductivity changes). With certain assumptions solving this inverse problem can be described by the following equation (Schullcke et al., 2016):

$$\hat{\mathbf{x}} = (\mathbf{J}^t\mathbf{J} + \lambda^2\mathbf{R}^t\mathbf{R})^{-1}\mathbf{J}^t\mathbf{y} = \mathbf{B}\mathbf{y} \quad (1)$$

where $\hat{\mathbf{x}}$ are the calculated conductivity changes and $\mathbf{y}$ the measured voltage changes (Schullcke et al., 2016; Adler and Boyle, 2017). The Jacobian matrix $\mathbf{J}$ relates the voltage changes to conductivity changes and the hyperparameter λ weighs the regularization matrix $\mathbf{R}$ (Schullcke et al., 2016; Adler and Boyle, 2017). $\mathbf{B}$ is the calculated reconstruction matrix (Schullcke et al., 2016; Adler and Boyle, 2017). The equation uses conductivity and voltage changes because difference imaging is applied. Difference imaging describes the process of relating each measurement frame to a reference frame (Adler and Boyle, 2017). Generally speaking, difference imaging is more robust because the influences of geometry variations, electrode movements,

⋆ Research funding: This research was partially supported by the German Federal Ministry of Education and Research (MOVE, Grant 13FH628IX6) and the grant AIRLobe (32-7545.220/42/1) funded by "Innovative Projects" MWK-BW

10.1016/j.ifacol.2023.10.469

etc. on the reconstruction are smaller (Frerichs et al., 2017).

Additionally to monitoring respiration, EIT might be capable of monitoring perfusion of the lungs and heart activity itself because some conductivity changes are assumed to be related to them (Putensen et al., 2019). This could be clinically relevant for monitoring the ventilation-perfusion ratio (V/Q ratio) of the lungs. A mismatch between ventilation and perfusion is indicated by a V/Q-ratio larger or smaller than 1 (Silbernagl and Draguhn, 2018).

It is necessary to separate the respiration and perfusion signals to assess the V/Q-ratio if only EIT is used. Although several separation techniques have been published in recent years, methods solely based on signal processing (i. e. without contrast agents or similar) like filtering, principle component analysis (PCA) or ECG-gating have not reached clinical relevance yet (Putensen et al., 2019; Frerichs et al., 2017; Battistel et al., 2021).

We recently proposed a different approach, which implements harmonic analysis for separation of respiration and perfusion in EIT (Battistel et al., 2021). Simply speaking, it fits the different harmonics of respiration and perfusion with Hermite functions in the frequency domain and then reconstructs them separately with Hermite polynomials in the time domain. Advantageously, an overlap of respiratory harmonics into the frequency range of cardiac activity will not influence the separation as long as the basis frequency are no integer multiples or close to it. With a simulation study it has already been shown that harmonic analysis might be capable of delivering reliable and precise separation results (Stein et al., 2022).

In this paper, we investigate whether different image reconstruction algorithms and regularization techniques change the separation results delivered by harmonic analysis. A comparison between the following algorithms is made:

(1) Algorithm used in the EIT Device PulmoVista ® 500 manufactured by Dräger (Dräger)
(2) Gauss-Newton with $R = R_{Laplace}$ (GN Laplace)
(3) Gauss-Newton with $R = R_{Tikhonov}$ (GN Tikhonov)
(4) Gauss-Newton with $R = R_{NOSER}$ (GN NOSER)
(5) Graz consensus reconstruction algorithm for EIT (GREIT)

The separation is conducted on the global (sum of all pixels over time) and the pixel-wise impedance values for each algorithm. The dataset was collected on COVID-19 patient, who was deeply sedated and supported with pressure controlled mechanical ventilation. We decided to use clinical instead of simulated data because clinical data offers more complexity. Also a relative comparison between the reconstruction algorithms is enough for the investigation whether they deliver different separation results.

2. HARMONIC ANALYSIS

The harmonic analysis approach separates respiration and perfusion by firstly fitting their harmonics with Hermite functions in the frequency domain (Battistel et al., 2021). Hermite functions are recursively calculated as

$$\begin{aligned} \Psi_0(x) &= \pi^{-\frac{1}{4}} e^{-\frac{1}{2}x^2} \\ \Psi_1(x) &= \pi^{-\frac{1}{4}} \sqrt{2}\, x e^{-\frac{1}{2}x^2} \\ \Psi_{p+1}(x) &= \sqrt{2/(p+1)}\, x\, \Psi_p(x) \\ &\quad -\sqrt{p/(p+1)}\, \Psi_{p-1}(x) \end{aligned} \tag{2}$$

Secondly, the calculated coefficients from the fitting process are used in the time domain for reconstructing the separated signals with Hermite polynomials. Hermite polynomials can be recursively calculated as

$$\begin{aligned} H_0(x) &= 1 \\ H_1(x) &= 2x \\ H_{p+1}(x) &= 2xH_p(x) - 2pH_{p-1}(x) \end{aligned} \tag{3}$$

Hermite functions have the important property of being eigenvectors of the Fourier transformation, which means they have the same shape in the frequency and the time domain. Therefore, the coefficients calculated in the fitting process in the frequency domain can simply be used for reconstruction in the time domain. To use Hermite functions in the frequency domain a Gaussian window function is employed. This is used to "squeeze" the peak intensity.

The harmonic analysis can then be described by the following two equations, which represent the separated respiration and perfusion:

$$\begin{aligned} \hat{y}_r(t) = \sum_{p=0}^{N_p} \sum_{n=1}^{N_h} (\; & \hat{\theta}^g_{nf_r,p} \cos(2\pi n f_r t) - \\ & \hat{\theta}^h_{nf_r,p} \sin(2\pi n f_r t)) b_p(t) \end{aligned} \tag{4}$$

$$\begin{aligned} \hat{y}_p(t) = \sum_{p=0}^{N_p} \sum_{n=1}^{N_h} (\; & \hat{\theta}^g_{nf_p,p} \cos(2\pi n f_p t) - \\ & \hat{\theta}^h_{nf_p,p} \sin(2\pi n f_p t)) b_p(t) \end{aligned} \tag{5}$$

where $\hat{y_r}$ describes the reconstructed respiration and $\hat{y_p}$ the reconstructed perfusion signal. f_r and f_p respectively describe the basis frequencies of respiration and perfusion and $\hat{\theta}$ the calculated coefficients from the fitting process. The basis functions $b_p(t)$ are shifted Hermite polynomials. N_p describes how many coefficients are used in the fitting process and N_h how many harmonics are actually fitted.

For more details please refer to the original paper (Battistel et al., 2021).

3. RECONSTRUCTION ALGORITHMS

3.1 Dräger

The Dräger algorithm uses a linearized Newton-Raphson method (a.k.a. Newton's method) to reconstruct the conductivity changes based on an FEM model (Zhao et al., 2014). The exact algorithm is not known to the public because the PulmoVista ® 500 is a commercial device (Zhao et al., 2014).

3.2 GN Laplace

This algorithm uses the Gauss-Newton algorithm, which is based on Newton's method but solves a non-linear least squares problem. For regularization a Laplace filter is used,

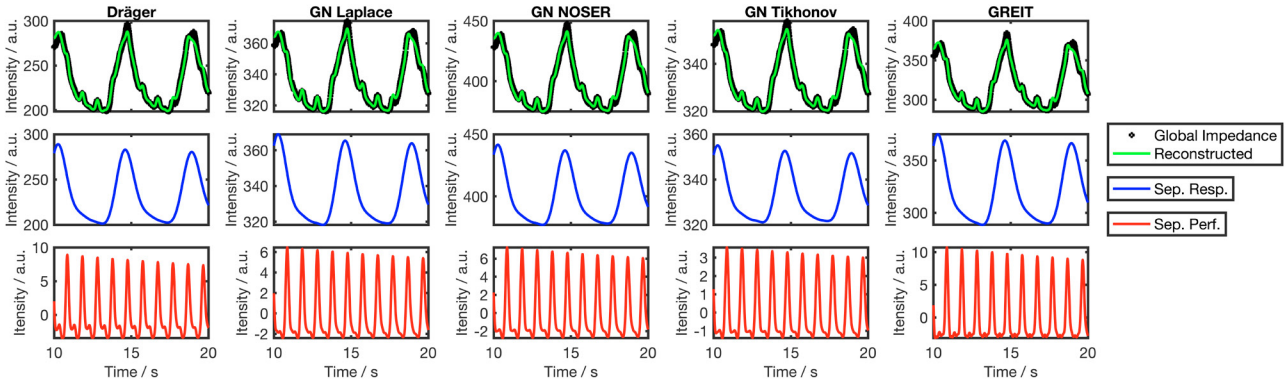

Fig. 1. Global impedance based separation results: It shows the original and reconstructed global impedance (first row), the separated respiration (second row) and the separated perfusion (third row)

which is a second order high pass filter and penalizes non-smooth solutions (Schullcke et al., 2016).

3.3 GN Tikhonov

With Tikhonov the regularization matrix $\mathbf{R}$ is set to the identity matrix $\mathbf{I}$ enforcing solutions with smaller norms (Schullcke et al., 2016).

3.4 GN NOSER

NOSER is a regularizer used with the Gauss-Newton algorithm. In this case the regularization matrix $\mathbf{R}$ is calculated as the diagonal of $\mathbf{J^tJ}$ (Cheney et al., 1990; Javaherian et al., 2013). As one can see, NOSER is the extension of Tikhonov as it weighs the diagonal matrix $\mathbf{I}$ with the FEM elements sensitivity represented by the Jacobian $\mathbf{J}$ (Adler et al., 2009; Adler and Boyle, 2017).

3.5 GREIT

The GREIT algorithm introduces training data as prior information to the image reconstruction process (Adler et al., 2009; Adler and Boyle, 2017).

4. METHOD

The comparison is based on a retrospective clinical EIT dataset of a COVID-19 patient, who was mechanically ventilated and sedated (Lovas et al., 2022). The study was approved by the Human Investigation Review Board of the University of Szeged (approval number 67/2020-SZTE) and the trial was registered under NCT04360837 (ClinicalTrials.gov). The measurements were conducted at a frame rate of 50 Hz with the PulmoVista ® 500 manufactured by Drägerwerk AG & Co. KGaA. The raw voltage data and the reconstructed images were both provided by the device.

The image reconstructions based on the raw voltage data were carried out in Matlab 2019a (Mathworks, Natick, MA) with the EIDORS toolbox (Version 3.10) (Adler and Lionheart, 2006) including Netgen. Netgen was used for building the finite element method (FEM) models to reconstruct on (Schöberl, 1997). The Dräger reconstruction was directly retrieved from the device. Matlab 2021a (Mathworks, Natick, MA) was used for running the separation. Harmonic analysis was performed following our previous work (Battistel et al., 2021).

The different hyperparameters λ for each reconstruction algorithm were chosen to result in a noise figure (NF) of 0.5 following the approach of Adler and Guardo (1996) and are listed in table 1. The GREIT algorithm does not have a hyperparameter but still adapts itself to the NF of 0.5 by changing the weight given to the training data (Adler et al., 2009).

Table 1. Hyperparameters with $NF = 0.5$

Reconstruction algorithm	Hyperparameter
GN Laplace	0.0227
GN Tikhonov	0.0240
GN NOSER	0.0770

We applied the harmonic analysis on the global and the pixel-wise impedance for each reconstruction algorithm. Three respiration and four perfusion related harmonics were fitted with two coefficients each. The Gaussian window was assigned a width of two.

5. RESULTS

In Fig. 1 the separation results of the global impedance are presented based on the different reconstruction algorithms. The global impedance curve in the first row was sufficiently fitted in all five cases. The sum square mean (SSM) of the fitting process is given in table 2. It is clearly visible, that the intensity between all algorithms varies. Still, the overall shapes of the reconstructed signals are comparable. Also the separated respiration signal is similar among the five algorithms but again differing in intensity. Interestingly, the separated perfusion signals do not only differ in intensity but also in shape. This is especially visible in the lower intensity region of the curves.

Table 2. SSM of global impedance fitting

Reconstruction algorithm	SSM
Dräger	0.0043
GN Laplace	0.0015
GN Tikhonov	0.0024
GN NOSER	0.0006
GREIT	0.0042

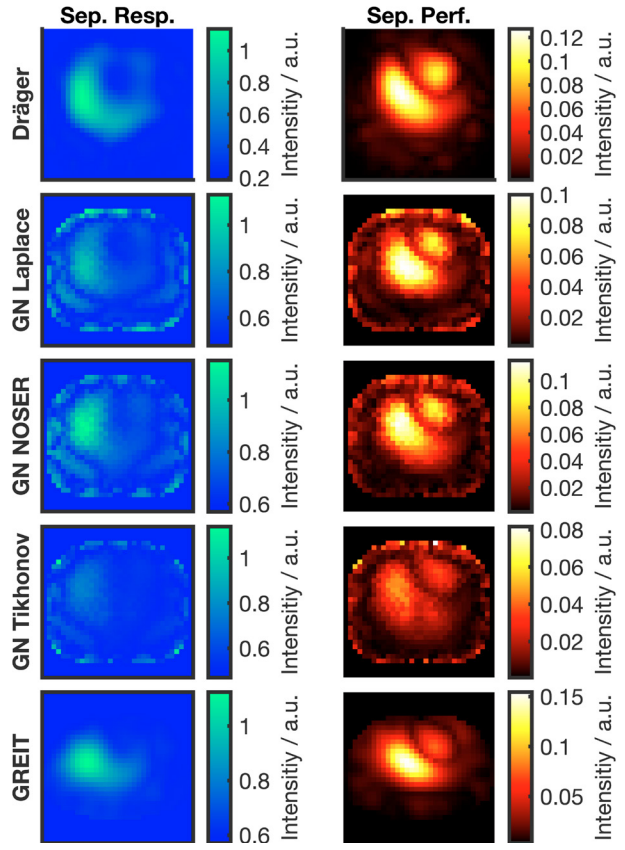

Fig. 2. Pixel-wise separation results of respiration (left column) and perfusion (right column) depicted as maximum images

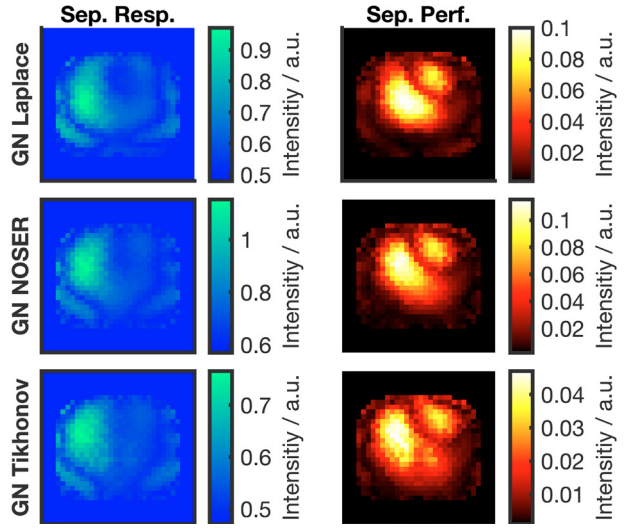

Fig. 3. Pixel-wise separation results of respiration (left column) and perfusion (right column) depicted as maximum images (GN algorithms, cropped)

In Fig. 2 the pixel-wise separation results of respiration and perfusion are depicted as maximum images (maximum value of each pixel). Here the differences between the reconstruction algorithms are obvious. Overall, the separation results of Dräger and GREIT are smoother and less noisy than the results of GN Laplace, GN Noser, and GN Tikhonov. Additionally, the signal intensity of Dräger and GREIT is concentrated in the expected regions of the heart and lungs and not at the boarders of the FEM model.

The separated respiration of the Dräger reconstruction in Fig. 2 shows the highest activity in the right lung (left side of the image) and some lower activity in the left lung. GN Laplace and GN NOSER show similar results. For GN Tikhonov the activity in the lungs is almost invisible due to strong boundary artifacts. The GREIT separation results emphasize the right lung but are squeezed in the y-dimension. All separated respiration images show some additional activity around the lungs. However, these additional activities are most prominent in GN Laplace, GN NOSER and GN Tikhonov.

The separated perfusion images in Fig. 2 show similar shapes for all reconstruction algorithms with one smaller round shape and one larger banana-shaped area being present. The smaller round shape likely represents the hearts activity while the banana-shaped area might relate to the perfusion of the lungs. Overall, Dräger and GN Laplace show the highest similarity, followed by GN NOSER and GREIT. However, the center of highest activity of GN NOSER is shifted towards the top, while GREIT shows a very smooth and squeezed separation result. GN Tikhonov shows the highest activity at the borders of the FEM model, where one would expect the electrodes and only light activity in the lung and heart area. Still, the shapes present in GN Tikhonov are similar to the others as shown with Fig. 3. In Fig. 3 we cropped out the boundary artifacts and then recalculated the color scale for the GN algorithms.

6. DISCUSSION

As shown with the results, different image reconstruction methods deliver different separation results when harmonic analysis is applied especially in the pixel-wise separation. The differences among the reconstruction algorithms in the separation of the global impedance however were only visible marginally. In the pixel-wise separation GN Tikhonov pushed the noise to the boundaries of the FEM model, which is a disadvantage of the algorithm mentioned in the literature (Adler et al., 2009; Adler and Boyle, 2017). NOSER, which is an extension of Tikhonov, delivered a more reliable reconstruction and also clearer separation results (Adler et al., 2009; Adler and Boyle, 2017). The Dräger and GREIT reconstruction algorithms commonly produce rather smooth images (Adler et al., 2009), which is also visible in the separation results (see Fig. 2).

Nevertheless, this investigation has limitations: First, the FEM models of Dräger and GREIT do not match the FEM models used for the GN based algorithms. Drägers FEM model is not publicly available and we were not able to implement the GN based algorithms with the FEM model used by GREIT. This also explains why the separation results based on GREIT are squeezed as GREITs FEM model is smaller in the y-dimension. Second, we applied the NF-approach for calculating the hyperparameter λ. However, the Dräger device does not use this approach and, therefore, comparability between the Dräger algorithm and the others is limited in this case. Third, we are aware that other reconstruction algorithms and regu-

larization techniques like the D-bar method exist but were not included in this paper. Last, we cannot compare the separations quantitatively because no additional perfusion or ventilation data is available.

7. OUTLOOK

We conclude that the harmonic analysis approach is dependent on the image reconstruction algorithm applied beforehand. The differences were small but still observable and, therefore, we recommend the development of a method where the harmonic analysis approach can be applied before image reconstruction. More precisely, we suggest applying this novel separation technique on the raw voltage data and then, afterwards, carry out image reconstruction for respiration and perfusion independently. This could also open the door for new research areas investigating whether respiration and perfusion might actually benefit from different image reconstruction algorithms.

REFERENCES

Adler, A. and Guardo, R. (1996). Electrical impedance tomography: regularized imaging and contrast detection. *IEEE transactions on medical imaging*, 15(2), 170–179. doi:10.1109/42.491418.

Adler, A., Arnold, J.H., Bayford, R., Borsic, A., Brown, B., Dixon, P., Faes, T.J.C., Frerichs, I., Gagnon, H., Gärber, Y., Grychtol, B., Hahn, G., Lionheart, W.R.B., Malik, A., Patterson, R.P., Stocks, J., Tizzard, A., Weiler, N., and Wolf, G.K. (2009). Greit: a unified approach to 2d linear eit reconstruction of lung images. *Physiological Measurement*, 30(6), S35–S55. doi:10.1088/0967-3334/30/6/S03.

Adler, A. and Boyle, A. (2017). Electrical impedance tomography: Tissue properties to image measures. *IEEE transactions on bio-medical engineering*, 64(11), 2494–2504. doi:10.1109/TBME.2017.2728323.

Adler, A. and Lionheart, W.R.B. (2006). Uses and abuses of eidors: an extensible software base for eit. *Physiological measurement*, 27(5), S25–42. doi:10.1088/0967-3334/27/5/S03.

Battistel, A., Chen, R., Hallemans, N., Pintelon, R., Lataire, J., and Möller, K. (2021). Harmonic analysis for the separation of perfusion and respiration in electrical impedance tomography. *IFAC-PapersOnLine*, 54(15), 281–286. doi:10.1016/j.ifacol.2021.10.269.

Cheney, M., Isaacson, D., Newell, J.C., Simske, S., and Goble, J. (1990). Noser: An algorithm for solving the inverse conductivity problem. *International Journal of Imaging Systems and Technology*, 2(2), 66–75. doi:10.1002/ima.1850020203.

Frerichs, I., Amato, M.B.P., van Kaam, A.H., Tingay, D.G., Zhao, Z., Grychtol, B., Bodenstein, M., Gagnon, H., Böhm, S.H., Teschner, E., Stenqvist, O., Mauri, T., Torsani, V., Camporota, L., Schibler, A., Wolf, G.K., Gommers, D., Leonhardt, S., and Adler, A. (2017). Chest electrical impedance tomography examination, data analysis, terminology, clinical use and recommendations: consensus statement of the translational eit development study group. *Thorax*, 72(1), 83–93. doi:10.1136/thoraxjnl-2016-208357.

Javaherian, A., Movafeghi, A., and Faghihi, R. (2013). Reducing negative effects of quadratic norm regularization on image reconstruction in electrical impedance tomography. *Applied Mathematical Modelling*, 37(8), 5637–5652. doi:10.1016/j.apm.2012.11.022.

Lovas, A., Chen, R., Molnár, T., Benyó, B., Szlávecz, Á., Hawchar, F., Krüger-Ziolek, S., and Möller, K. (2022). Differentiating phenotypes of coronavirus disease-2019 pneumonia by electric impedance tomography. *Frontiers in Medicine*, 9. doi:10.3389/fmed.2022.747570. URL `https://doi.org/10.3389/fmed.2022.747570`.

Putensen, C., Hentze, B., Muenster, S., and Muders, T. (2019). Electrical impedance tomography for cardiopulmonary monitoring. *Journal of clinical medicine*, 8(8). doi:10.3390/jcm8081176.

Schöberl, J. (1997). Netgen an advancing front 2d/3d-mesh generator based on abstract rules. *Computing and Visualization in Science*, 1(1), 41–52. doi:10.1007/s007910050004.

Schullcke, B., Gong, B., Krueger-Ziolek, S., Soleimani, M., Mueller-Lisse, U., and Moeller, K. (2016). Structural-functional lung imaging using a combined ct-eit and a discrete cosine transformation reconstruction method. *Scientific reports*, 6, 25951. doi:10.1038/srep25951.

Silbernagl, S. and Draguhn, A. (2018). *Taschenatlas Physiologie*. Thieme, Stuttgart, 9. vollständig überarbeitete auflage edition. URL `http://nbn-resolving.org/urn:nbn:de:bsz:24-epflicht-1929898`.

Stein, E., Chen, R., Battistel, A., and Moeller, K. (2022). Separating respiration and perfusion in eit: Harmonic analysis on 2d-thorax simulation. *Current Directions in Biomedical Engineering*, 8(2), 785–788. doi:10.1515/cdbme-2022-1200.

Zhao, Z., Frerichs, I., Pulletz, S., Müller-Lisse, U., and Möller, K. (2014). The influence of image reconstruction algorithms on linear thorax eit image analysis of ventilation. *Physiological measurement*, 35(6), 1083–1093. doi:10.1088/0967-3334/35/6/1083.